International Journal of Mechanical, Industrial and Aerospace Sciences
ISSN: 2517-9950
Vol:14, No:12, 2020

Computational Fluid Dynamics Analysis and Optimization of the Coanda Unmanned Aerial Vehicle Platform

Nigel Q. Kelly, Zaid Saddiqi, Jin W. Lee

Abstract**—**It is known that using Coanda aerosurfaces can drastically augment the lift forces when applied to an Unmanned Aerial Vehicle (UAV) platform. However, Coanda saucer UAVs, which commonly use a dish-like, radially-extending structure, have shown no significant increases in thrust/lift force and therefore have never been commercially successful: the additional thrust/lift generated by the Coanda surface diminishes since the airstreams emerging from the rotor compartment expand radially causing serious loss of momentums and therefore a net loss of total thrust/lift. To overcome this technical weakness, we propose to examine a Coanda surface of straight, cylindrical design and optimize its geometry for highest thrust/lift utilizing computational fluid dynamics software ANSYS Fluent®. The results of this study reveal that a Coanda UAV configured with 4 sides of straight, cylindrical Coanda surface achieve an overall 45% increase in lift compared to conventional Coanda Saucer UAV configurations. This venture integrates with an ongoing research project where a Coanda prototype is being assembled. Additionally, a custom thrust-stand has been constructed for thrust/lift measurement.

Keywords**—**CFD, Coanda, Lift, UAV.

I. Introduction

SINCE the early 2010's, recreational use of unmanned aerial vehicle (UAV) systems have been popular. In recent years, the recreational drone market has exploded, particularly with the vertical takeoff and landing (VTOL) variety, as they require no runway for takeoff and landing. These VTOL UAVs, whether commercial or not, have been dominated by multi-rotor designs. The major components of these drones are a frame, multiple propellers, and the same number of motors. The use of external propellers is a two-edged sword: they are relatively simple and less expensive to build than conventional gas turbine engines. However, a severe disadvantage in terms of propulsion efficiency has risen, since, in general, propellers are extremely inefficient due to their high aerodynamic/ viscous losses. As the rotational speed of the propeller increases, the viscous losses increase more severely since the intensity level of the induced turbulence increases exponentially [1], [2]. The inevitable inefficiencies commonly possessed by multi-rotor drones have enormously lowered their maneuvering capabilities: flight range, duration, and payload. It is no coincidence that most of today's drones are intended for short-range, light-duty missions such as video filming and racing [3].

Nigel Kelly is with the University of Arkansas at Little Rock, United States (e-mail: nqkelly@ualr.edu).

This paper examines an alternative class of VTOL UAVs called Coanda UAVs, which have the potential to significantly outclass multi-rotor designs. These 'flying saucers' have flight principles based on the Coanda effect and the Streamline Curvature theorem, otherwise known as Bernoulli's Theorem applied to an inviscid streamline in the normal direction. Ever since Henri Coanda, the father of the modern jet engine, filed his first patent in 1938 regarding a propulsion device using the "Coanda effect" [4], many variations of this device have been reported by various researchers around the world [5], [6]. The most common design is shown in Fig. 1.

Fig. 1 A typical Coanda Saucer UAV developed and tested by Jean-Louis Naudin. The diameter of the saucer is approximately 60 cm [11]

The name 'saucer' originates from the bottom portion of the device, which is a unique, convex, dish-like structure known as a Coanda surface. By directing the flow of air from a propeller over this Coanda surface, a negative pressure gradient forms, resulting in additional lift generated. In theory,

the direct thrust from the propeller in the gravity direction is then augmented by this additional lift force. Methods have been developed that can analytically compute the lift and thrust from a typical Coanda UAV [7]-[9]. Common Coanda UAVs have flow directed radially outwards from an orifice and, due to the Coanda effect, are vectored in the direction of Coanda curvature. It turns out that this behavior is highly influenced by the height, h, of the airstream emerging from the orifice preceding the Coanda surface and the radius of curvature, R, of the Coanda surface, as shown in Fig. 2. Another key influence is the form or 2-dimensional profile of the Coanda surface. Numerical studies have only begun to explore the effects of Coanda jet attachment for differing Coanda curvature profile forms and convexities for a radial Coanda surface [10], [9]. This paper examines a Coanda curvature of circular shape as a baseline design factor due to its direct applicability to the Streamline Curvature Theorem.

II. Background

In a typical Coanda Saucer UAV, the airstreams, accelerated by an external rotor at the top portion, move along its curved surface. Since it is convex, the pressure immediate to the Coanda surface is lower than ambient air pressure. This low-pressure region acting on the surface creates additional thrust/lift forces against the force of gravity. The Bernoulli theorem, in normal direction to the streamline, states that the pressure gradient is proportional to the square of an airstream's velocity and inversely proportional to the streamline's radius of curvature, as is shown in (1), where $\partial p/\partial n$ is the change in pressure with respect to the normal direction, V is the velocity of the fluid, ρ is the fluid density, and R is the radius of curvature.

$$\frac{\partial p}{\partial n} = \rho \cdot \frac{V^2}{R} \tag{1}$$

Hence, to maximize the additional pressure gains from the Coanda surface, a high air-velocity and small radius of curvature are required. Equation (1) can then be simplified into (2), where ∂n becomes the orifice height, h, and ∂p becomes Δp, the change in pressure.

$$\Delta p = \rho \cdot V^2 \cdot \left(\frac{h}{R}\right) \tag{2}$$

It should be stressed that decreasing the radius of curvature also reduces the surface area of the Coanda surface, which affects the overall lift force. In this case, lift forces due to pressure changes can be derived from (3), where A_s is the active surface area of which the Coanda jet is in contact, and F is the force generated from change in pressure. Hence, lift force is directly proportional to Coanda surface area and indirectly proportional to the radius of curvature. These competing parameters must be balanced in order to achieve optimal thrust/lift.

$$F = \Delta p \cdot A_s \tag{3}$$

It can be shown that Coanda saucer UAV's share an intrinsic weakness: the additional thrust/lift generated by the saucer-like Coanda surface swiftly diminishes since the airstreams emerging from the rotor compartment *expand radially* causing serious loss of momentums and therefore a *net loss* of total thrust/lift. To overcome this flaw, a straight, cylindrical Coanda design would maintain the active surface area of the Coanda surface constant with respect to the radius of curvature, reducing momentum losses. In this paper, a straight cylindrical Coanda surface profile, intended for use with a 25.4 cm (9 in) propeller, is examined in detail to identify the geometries resulting in highest thrust/lift. Insights gathered from this research will be applied to a 4-sided straight cylindrical Coanda flight saucer which has a general cross section shown in Fig. 2. This 2-dimensional profile, shown in bold, can be applied to both design concepts, radial and 4-sided cylindrical. To accomplish the study of these design models, fluid simulations using ANSYS Fluent® are used alongside non-dimensional parameters generated from the Buckingham Pi theorem method.

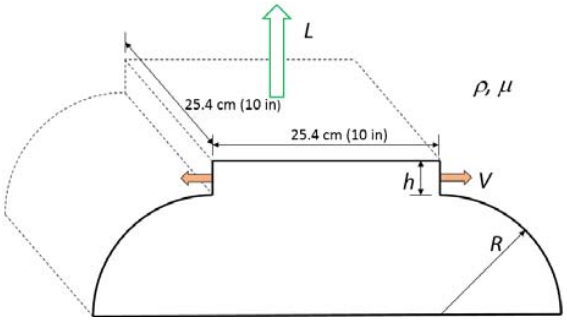

Fig. 2 The Coanda UAV 2-dimensional profile, with depth extending into the page. Note that only 2 sides are shown for illustration purposes

The 2-dimensional analysis starts with identification of the fundamental parameters used to generate non-dimensional Pi terms. The parameters selected are noted in Table I.

TABLE I
Fundamental Parameters Used to Form Pi Terms

Symbol	Quantity	Units
L	Lift Force	N
μ	Dynamic Viscosity	N·s/m^2
ρ	Density	kg/m^3
V	Orifice Velocity	m/s
h	Orifice Height	m
R	Radius of Curvature	m

The Pi terms created are the ratio of orifice height to the radius of curvature, h/R, Reynolds Number, Re, and Lift Coefficient, $\mathcal{L}$. Using these non-dimensional parameters and targeting a specific range of radii, a broad review of Coanda UAV geometries is cultivated. The scope of this paper is limited to examining Coanda surfaces with radii of 3 cm, 5 cm, 7 cm of straight cylindrical design.

III. Assumptions

For the simulations, it is assumed that the environment is under standard temperature and pressure conditions. The UAV is considered of a certain size which can be enclosed inside a 100 cm cubic volume. This limits our scope to simulating Coanda surfaces with radii ranging from 3 cm to 11 cm. For simplicity of simulation, it is also assumed the velocity emerging from the orifice is homogeneous. To gain an appreciative picture of Reynold's number impact on the flow behavior, velocities of 30 m/s, 40 m/s, 50 m/s are used for the orifice velocity, V. The critical Reynolds number is calculated using a characteristic length of $\pi R/2$, which is a circle's circumference divided by 4. It is important to note that some of the subsequent flow situations result in a calculated Reynold's number below the critical amount, indicating a laminar flow. However, given the nature of the simulations, it is assumed that all simulations are turbulent. K-ω SST turbulence model was used since it combines the near wall advantages of the K-ω model and free stream advantages of the K-ε model [12]. Due to the symmetric nature of the 2-dimensional profiles, centerline symmetry was employed in the simulations to reduce computational costs.

IV. Methodology

Gathering data requires separate techniques for lift force, direct thrust, and validation. Extracting the lift force information from ANSYS Fluent® is relatively straight-forward. By navigating to Reports → Forces, then selecting the direction vector in the gravity direction and selecting the Coanda wall boundary, lift forces can then be printed to the console. However, obtaining information on direct thrust and validation require more effort.

Direct thrust can be ascertained by using a control volume and linear momentum equation approach [1], [8].

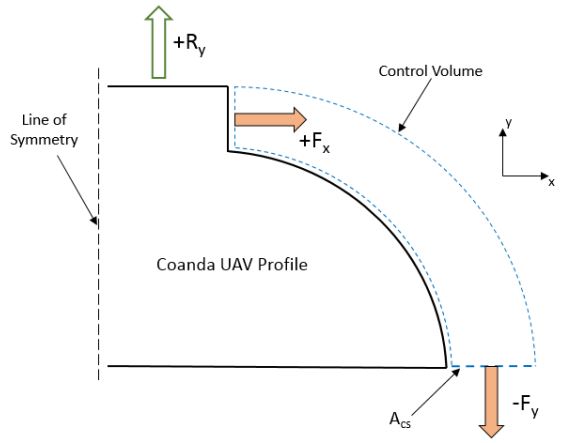

Fig. 3 Control Volume and Linear momentum approach to calculating direct thrust of the Coanda Surface

As shown in Fig. 3, forces acting in the x-direction cancel due to symmetry, leaving the negative y-forces behind. This, in effect, causes a reaction force in positive y-direction, which results in the craft ascent. As derived from the linear momentum direction, the equation to calculate direct thrust is thus:

$$F = \dot{m} \cdot V = (\rho \cdot A_{cs} \cdot V_y) \cdot V_y = \rho \cdot A_{cs} \cdot V_y^{\,2} \qquad (2)$$

where A_{cs} is the area of the control surface from which the Coanda jet is leaving, V_y is the area-weighted average velocity in the y-direction of the Coanda jet, and ρ is the density of the Coanda jet. To calculate direct thrust of the Coanda jet, A_{cs} and V_y were estimated using features within ANSYS Fluent. First, from the post-processing velocity contours, a horizontal line is drawn extending from the end of the Coanda surface to the conclusion of the Coanda jet boundary. This line is then used with Surface Integrals (Results → Reports) to compute A_{cs} and V_y.

V. Meshing Process

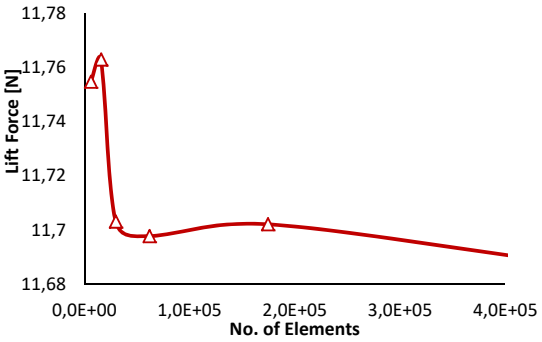

Fig. 4 Mesh Dependency Study

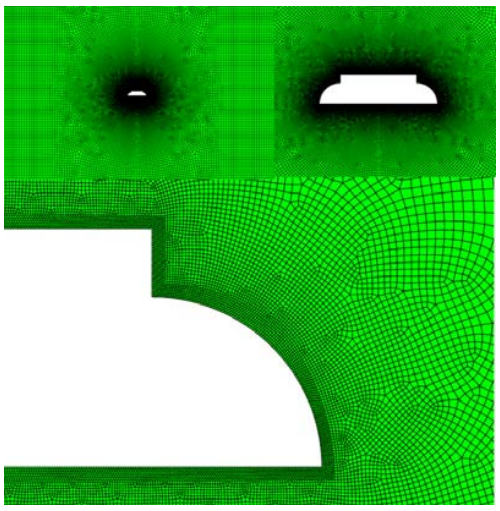

Fig. 5 Mesh used for simulation. Minimum Orthogonal Quality = 7.04319e-01, Maximum Aspect Ratio = 2.76836e+00

Using ANSYS Meshing, a Multizone Quad/Tri method was used along with inflation and edge-sizing features around the Coanda profile with sizing equal to 1 mm. The free face meshing was designated as 'all quad' and the sizing growth of

the overall mesh rate varies from 1.025 to 1.04. The mesh generated from this method concentrates around the Coanda UAV profile and gradually expands its element size as distance from the Coanda profile increases outward. The overall dimensions of the fluid container are 3 m horizontal by 10 m vertical.

To validate the mesh, a mesh dependency study was conducted. This study compares the lift result from meshes which have varying element ranges. To lower the computation cost, mesh dependency studies are employed to identify the lowest number of mesh elements required in order to obtain a result which does not change drastically given a radical change in the number of elements. To that end, meshes having elements between 50,000 to 65,000 elements were used in this study.

VI. Results

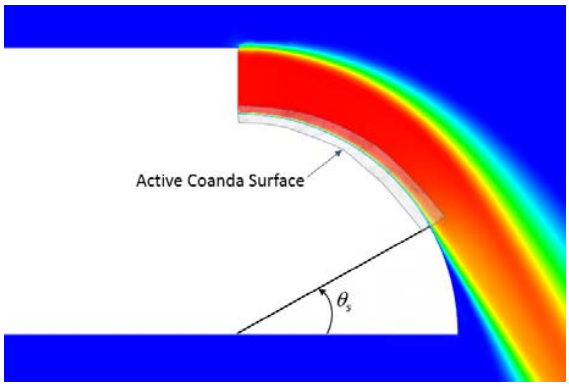

Fig. 6 Velocity contours of the Coanda 2-d profile with separation. *(h = 2.1 cm, R = 7 cm, V = 50 m/s)*

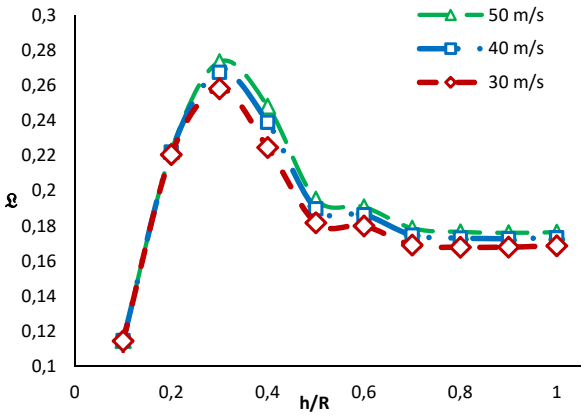

Fig. 7 Non-dimensional Study of the Coanda Saucer UAV performance with varying velocities and h/R ratio (R = 7 cm)

Shown in Fig. 7 is a plot for a straight Coanda surface with radius of curvature, R, equal to 7 cm. The lift coefficient rises sharply as h/R is low, peaking around $h/R = 0.3$ then drops and levels out at ($0.35 < h/R \leq 1.0$). This is caused by the Coanda jet separating from the Coanda surface, as shown in Fig. 6. This decreases the 'active' Coanda surface area which is generating lift. θ_s is the angle at which the separation occurs. Separation angle increases as h/R increases. Results for radius of curvature, R, equal to 3 cm and 5 cm show a similar story.

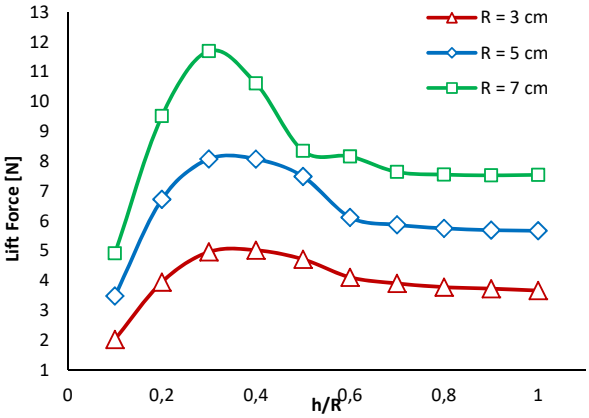

Fig. 8 Comparison of Coanda UAV profile with different radii of curvature

In Fig. 8, different radii of straight Coanda surfaces are compared. As the radius of curvature is increased, the lift force increases correspondingly, which is opposite to what we anticipated from Bernoulli theorem. This implies that even though the pressure gradient decreases with an increasing radius of curvature, the net lift force induced by the negative pressure will be greater due to a larger overall surface area.

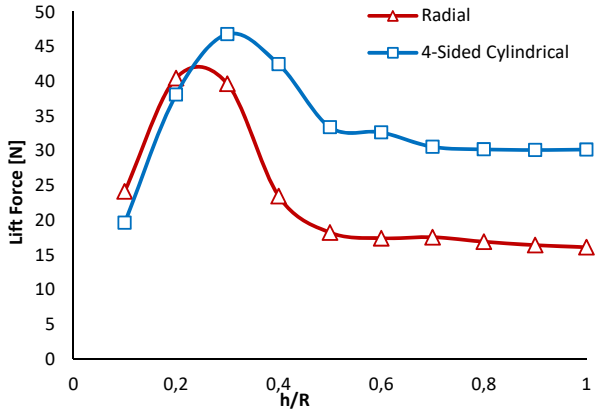

Fig. 9 Comparison of Radial vs 4-sided straight cylindrical Coanda surface configurations. (R = 7 cm, V = 50 m/s)

Next, we compare our proposed design with a conventional Coanda saucer, which has an identical dimension at radius of curvature of 7 cm. Multiplying the lift force generated from this Coanda surface by 4 times would give us the approximate amount of lift force for a 4-sided cylindrical design. In Fig. 9, results of the 4-sided cylindrical configuration are compared with those of a conventional radial configuration. As shown, the radial configuration shows some advantages at lower h/R ratios. However, its peak h/R ratio results in lift force 10% lower than lift force resulting from the peak h/R of the 4-sided

cylindrical configuration. Peak *h/Rs* for the radial configuration and 4-sided straight cylindrical configuration are approximately 0.25 and 0.30, respectively. Overall, the 4-sided cylindrical configuration outperforms the radial configuration, according to our simulations. Comparing the average lift forces of each configuration with a range of ($0.10 < h/R \leq 1.0$) indicates a 45% increase in lift of the 4-sided straight cylindrical design over the radial design.

VII. Validation

Validation of the results is slightly complex. This technique focuses on the pressure gradient resulting from the Coanda effect along the Coanda surface.

Validation of the results is a correlation between theoretical estimation of the pressure gradient, $\partial p/\partial n$, and the simulated pressure gradient found in the simulation. Recalling (1), the Streamline Curvature theorem states that the pressure gradient, $\partial p/\partial n$, is directly proportional to the density of the fluid multiplied by the square of the fluid's velocity, divided by the radius of the streamline's curvature.

To calculate the theoretical $\partial p/\partial n$, the tangential velocity, V_t, must first be extracted from the post-processing results from the simulations. This was done by first standardizing a constant angle $\phi = 45°$ from which to read V_t. ϕ is defined as the angle between the horizontal and an arbitrary point along the Coanda surface. In the pressure contours of ANSYS Fluent®'s post-processing section, a line was utilized along this angle extending from the Coanda surface to a standardized distance of $\sqrt{2}$ mm. This line is identified as the $\partial p/\partial n$ line from which the tangential velocity is extracted from the simulations. From this point, theoretical estimation of the pressure gradient can be evaluated.

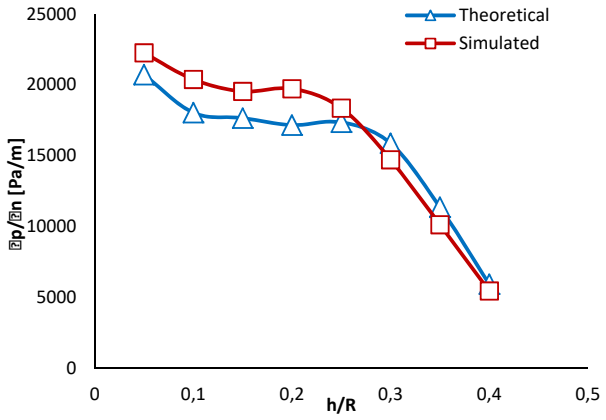

Fig. 10 Validation results comparing theoretical pressure gradient with simulated pressure gradient

The simulated pressure gradient is extracted from Fluent's post-processing by using a plotting technique. This is done by navigating to Results → Plots in Fluent's post processing section, selecting the [1 1] direction vector corresponding to the standardized ϕ direction, and plotting the static pressure along the $\partial p/\partial n$ line. This plot was then extracted to an excel spreadsheet where the slope of the pressure change, which is also the pressure gradient, was approximated.

As Fig. 10 shows, the results of the pressure gradient, $\partial p/\partial n$, on each simulation correlate well with those of a calculated pressure gradient using the average tangential velocity extracted from the simulations. This shows that pressure gradients seen in the simulations have similar resemblance to results gathered from Bernoulli's theorem applied to a streamline in the normal direction.

Another method of validation involves the use of empirical equation (4)—found in literature [13]—which predicts the separation angle of a curved Coanda wall jet, based on $h/R > 0.10$ [13].

$$\theta_s = 6.69 \cdot \left(\frac{R}{h}\right)^{1.54} \quad (4)$$

Table II lists the flow separation angles predicted by this equation and compares those angles to the velocity contours result from ANSYS Fluent®. Using the flow separation angle defined Fig. 6, the resulting velocity contours approximate the predicted flow separation angles well.

TABLE II
Flow Separation Prediction

h/R	θ_s (degrees)	Velocity Contour
0.1	0.0	
0.2	10.2	
0.3	47.3	
0.4	62.6	
0.5	70.5	

VIII. Discussion

From the results, it is seen that lift coefficient rises independently if either radius of curvature, *R*, or orifice velocity, *V*, are increased. It is assumed that lift coefficient

will rise indefinitely as V rises. It is also shown that adjusting the orifice velocity, V, only scales the lift coefficient with no change in the overall behavior of the study. The limit to h/R is dictated by the amount of airflow the rotor can accelerate out of the orifice. At high h/R, the amount of airflow required for the rotor to move would exceed the limits of the rotor, assuming that orifice velocity V is constant and homogeneous. Given these practical constraints, it would be wise to design a Coanda saucer with ($0.10 < h/R \leq 0.35$). With these factors in mind, the selection of the amount of straight cylindrical Coanda surfaces is brought into question. 4 sides of the straight Coanda surface are selected for ease of horizonal translation. With the use of flaps or similar method, a potential 4-sided straight cylindrical Coanda UAV will easily have the means to move in all six directions of a 3-dimensional space by selective throttling of the Coanda jets.

IX. Conclusion

Great effort was put into mapping the behavior of a Coanda surface as the parameters, h, R, and V were changed using computational fluid dynamics software ANSYS Fluent®. Moreover, a technique based on the Streamline Curvature theorem for validating the results was presented. The results were also visually validated using an empirical equation found in literature which predicts the flow separation. Findings were displayed for a straight cylindrical Coanda surface with radii of 3 cm, 5 cm, and 7 cm. Straight and radial Coanda configurations were contrasted, displaying their respective peak h/R ratios. It was shown that the peak h/R of the 4-sided straight cylindrical configuration has an increase of 10% in lift force when compared to the radial configuration's peak h/R lift force. Additionally, when averaging the results, an overall increase in lift of 45% is noted for the 4-sided straight cylindrical configuration. Results vary slightly between different radii of curvature but the most optimal geometry for a Coanda UAV configuration has an h/R of in the range of ($0.25 < h/R < 0.35$), according to our simulations. This result, coupled with a 4-sided cylindrical Coanda configuration, is deemed to be a very efficient design for enhancing thrust/lift of a Coanda UAV platform.

References

[1] P. M. Gerhart, A. L. Gerhart, and J. I. Hochstein, *Fundamentals of Fluid Mechanics, 8th Edition*. 2016.

[2] A. Akturk and C. Camci, "Tip Clearance Investigation of a Ducted Fan used in VTOL UAVs PART 1 : Baseline Experiments and Compuational Validation," 2011.

[3] B. T. Fraser *et al.*, "Review on Progress and Application of Active Flow Control Devices - Coandă Effect on Unmanned Aerial Vehicles," *Retrieved Oct.*, vol. 3, no. 1, pp. 113–137, 2018, doi: 10.4995/var.2015.4366.

[4] H. Coanda, "Propelling Device," 2,108,652, 1938.

[5] F. Nedelcut, "Towards a new class of aerial vehicles using the coanda effect," *Univ. Galati*, 2008.

[6] O. Crivoi, I. Doroftei, and F. Adascalitei, "A Survey on Unmanned Aerial Vehicles Based on Coanda Effect," *Tehnomus*, no. 20, pp. 338–344, 2013.

[7] H. Djojodihardjo, R. I. Ahmed, and A. Yousefian, "An analysis on the lift generation for Coandə micro air vehicles," *Proceeding - ICARES 2014 2014 IEEE Int. Conf. Aerosp. Electron. Remote Sens. Technol.*, pp. 164–169, 2014, doi: 10.1109/ICARES.2014.7024387.

[8] R. I. Ahmed, A. R. Abu Talib, A. S. M. Rafie, and H. Djojodihardjo, "Aerodynamics and flight mechanics of MAV based on Coandă effect," *Aerosp. Sci. Technol.*, vol. 62, pp. 136–147, 2017, doi: 10.1016/j.ast.2016.11.023.

[9] N. Mirkov and B. Rasuo, "Maneuverability of an UAV with COANDA effect based lift production," *28th Congr. Int. Counc. Aeronaut. Sci. 2012, ICAS 2012*, vol. 3, pp. 1745–1750, 2012.

[10] N. Mirkov and B. Rašuo, "Numerical simulation of air jet attachment to Convex walls and application to UAV," *Lect. Notes Comput. Sci. Eng.*, vol. 108, pp. 197–207, 2015, doi: 10.1007/978-3-319-25727-3_15.

[11] "The GFS UAV Project, A coanda effect flying saucer tested by Jean-Louis Naudin." http://jlnlabs.online.fr/gfsuav/index.htm (accessed Jul. 26, 2020).

[12] C. D. Argyropoulos and N. C. Markatos, "Recent advances on the numerical modelling of turbulent flows," *Appl. Math. Model.*, vol. 39, no. 2, pp. 693–732, 2015, doi: 10.1016/j.apm.2014.07.001.

[13] V. Dragan, "A new mathematical model for high thickness coanda effect wall jets," *Rev. Air Force Acad.*, vol. 1, no. 1, pp. 23–28, 2013.